

Performance Analysis of Using Nanofluids in Microchannel Heat Sink in different Flow Regimes and its simulation using Artificial Neural Network

Hossein Shokouhmand, Mohammad Ghazvini, and Jaber Shabanian

Abstract— In this study, silicon microchannel heat sink (MCHS) performance using nanofluids as coolants was analyzed. The nanofluid was a mixture of nanoscale Cu particles and pure water with various volume fractions. Based on theoretical models and experimental correlations, the heat transfer and friction coefficients required in the analysis were used. The microchannel heat sink performances for a specific geometries with dimensions $W_{ch} = W_{fm} = 100 \mu\text{m}$ and $L_{ch} = 300 \mu\text{m}$ is examined. In this study, flow in laminar and turbulent regimes using the theoretic and experimental relations was investigated; moreover an artificial neural network (ANN) was used to simulate the MCHS having laminar flow with different circumstances and after that, the best geometry and volume fraction of nanofluid could be found based on minimum thermal resistance.

Index Terms— Artificial Neural Network, Laminar and Turbulent Flow Regimes, Microchannel Heat Sink, Nanofluid.

I. INTRODUCTION

The microchannel heat sink (MCHS) has received extensive study over the past two decades because of its capability to dissipate large amounts of heat from a small area [1]. Experimental studies have shown that the MCHS has several distinct features compared to conventional heat dissipating devices, i.e., very small size and volume per heat load, the ability to produce a very high heat transfer coefficient, and small coolant requirements [2]–[4]. In addition to experimental studies, heat transfer predictions and geometry optimizations based on theoretical analysis and numerical modeling were carried out extensively in previous investigations [5]–[7]. Shokouhmand and Bahrami [8] studied the effects of electrokinetic field on heat transfer through rectangular microchannels. Also Muzychka [9] have studied different geometries and ducts such as Circular tubes, Rectangular, Elliptic and Polygonal ducts.

The most frequently used coolants in the MCHS study were air, water, and fluorochemicals. One of the methods for enhancing heat transfer is the application of additives to the working fluids. Recent interest based on this concept focused on heat transfer enhancement using a nanofluid in which nanoscale metallic or nonmetallic particles are suspended in

the base fluids. Several experimental and analytical studies have shown that nanofluids have higher thermal conductivity than pure fluids and therefore great potential for heat transfer enhancement [10]–[12].

There have been relatively few studies on nanofluid flow and heat transfer characteristics as comparing with those of pure fluid [13]–[16]. These studies indicated that the heat transfer coefficient was greatly enhanced in the nanofluid flow. The enhancement depended on the Reynolds flow number, particle Peclet number, particle size and shape and particle volume fraction. They also found that nanoparticles did not cause an extra pressure drop.

Although limited data is available on nanofluid flow and heat transfer characteristics, it is believed that nanofluids are able to enhance heat transfer. In this study, performance of MCHS using nanofluids as working fluid is analyzed. The heat transfer and friction coefficients required in the analysis were based on the theoretical and experimental studies in both laminar and turbulent regimes.

Several studies were about developing models and methods of artificial networks [17]. Taking advantage of technique developed by Kolmogorov, Kurkova [18] provided a direct proof of the universal approximation capabilities of perceptron type network with two hidden layers. Lippmann [19] demonstrated the computational power of different neural net models and the effectiveness of simple error correction training procedures. Single and multi layer perceptrons, which can be used for pattern classification, are described as well as Kohonen's feature map algorithm, which can be used for clustering or as a vector quantizer. In this study, a multi layer perceptron (MLP) neural network is used.

II. ANALYTICAL MODELING

A. MCHS model

Fig. 1 shows the geometric configuration of a MCHS. The top surface is assumed to be insulated. The heat sink performance is commonly measured by its thermal resistance. Based on the theoretical analysis [5], it can be expressed as

$$R_{th} = \frac{T_{w,max} - T_{f,in}}{Q/(W_{hs} L_{hs})} = R_{fin} + R_{cap} + R_{con} = \frac{1}{Nuk_f} \frac{1 + \beta}{1 + 2\alpha\eta} \frac{2\alpha}{1 + \alpha} W_{ch} + \frac{L_{hs}}{C_{pf} \mu_f} \frac{2}{Re} \frac{1 + \beta}{1 + \alpha} + \frac{t_b}{k_s} \quad (1)$$

H. Shokouhmand is with the University of Tehran, Iran (corresponding author to provide phone: +982161114029; e-mail: hshokoh@ut.ac.ir).

M. Ghazvini, Jr., is with the University of Tehran, Iran (e-mail: mghazvini_1@yahoo.com).

J. Shabanian is with the Sharif University of Technology, Tehran, Iran (e-mail: shabanian_j@mehr.sharif.edu)

α , β , η , and Re are defined as

$$\alpha = \frac{L_{ch}}{W_{ch}}, \beta = \frac{W_{fin}}{W_{ch}}, \eta = \frac{\tanh(m\alpha)}{m\alpha}, Re = \frac{\rho_f u_m D_h}{\mu_f} \quad (2)$$

In (2), m , u_m and D_h are defined as

$$m = \sqrt{Nu \frac{1+\alpha}{\alpha\beta} \frac{k_f}{k_s}}, u_m = \frac{\dot{V}}{NW_{ch}L_{ch}}, D_h = \frac{2W_{ch}L_{ch}}{(W_{ch} + L_{ch})} \quad (3)$$

N in (3) is given as

$$N = \frac{W_{hs} - W_{fin}}{W_{ch} + W_{fin}} \quad (4)$$

A pumping power supply is required to drive the coolant in MCHS operation. It is the product of the pressure drop across the heat sink ΔP and volume flow rate \dot{V} , i.e.,

$$Pow = \dot{V} \cdot \Delta p = \dot{V} \left(\lambda \frac{L_{hs}}{D_h} \rho_f \frac{u_m^2}{2} \right) \quad (5)$$

In (5), the pressure drops at the channel inlet and exit were neglected because they are usually small compared to that in the microchannel. From (1) and (5), Nu and λ are two important parameters for MCHS performance in addition to the microchannel geometry. Both Nu and λ depend on the flow regime and type of coolant used.

B. Nusselt number and friction coefficient models

Assuming laminar and fully developed flow in the microchannel, λ correlation for pure fluid is given as [5],

$$\lambda Re = 4(4.7 + 19.64G) \quad G = \frac{\left(\frac{1}{\alpha}\right)^2 + 1}{\left(\frac{1}{\alpha} + 1\right)^2} \quad (6)$$

And for λ in turbulent flow and in macro scales

$$\lambda = \frac{0.3164}{Re^{0.25}} \quad (7)$$

Since there was no correlation for turbulent flow in micro scale, we use the macro scale correlation (7), for turbulent flow.

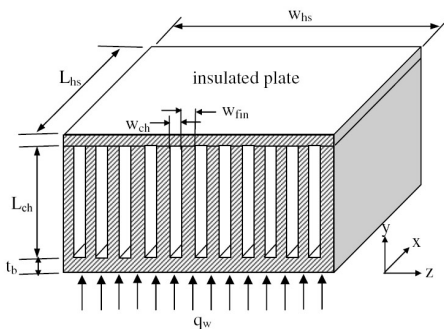


Fig. 1 Schematic diagram of the microchannel heat sink

As pointed out by Xuan and Roetzel [13], two approaches can be used to predict the heat transfer of nanofluids. The first approach is the conventional model that treats the nanofluid as a single-phase fluid. The heat transfer and friction coefficients are the same as those for pure fluid except that the nanofluid transport properties must be used. That is,

$$Nu = \frac{hD_h}{k_{nf}}, Re_{nf} = \frac{u_m \cdot D_h}{\nu_{nf}} \quad (8)$$

The nanofluid transport properties involved in the heat transfer and pressure drop calculations can be evaluated using the following expressions [13]

$$(\rho C_p)_{nf} = (1-\phi)(\rho C_p)_f + \phi(\rho C_p)_p \quad (9)$$

$$\mu_{nf} = \mu_f \frac{1}{(1-\phi)^{2.5}} \quad (10)$$

$$k_{nf} = k_f \frac{k_p + (SH-1)k_f - (SH-1)\phi(k_f - k_p)}{k_p + (SH-1)k_f + \phi(k_f - k_p)} \quad (11)$$

The second approach to describe the heat transfer for nanofluid flow is to treat the nanofluid as a two-phase mixture in which irregular and random movement of particle increases the heat exchanging rate. That is, thermal dispersion takes place in the nanofluid flow [17]. To take the thermal dispersion effect into account, it is better to describe the heat transfer based on experimental correlation. In the study by Xuan and Li [15], two formulas proposed to correlate the experimental data for nanofluid heat transfer coefficient (Nusselt number) in laminar and turbulent circular tube flow are given as

$$Nu_{nf} = 0.4328(1.0 + 11.285\phi^{0.754} Pe_d^{0.218}) Re_{nf}^{0.333} Pr_{nf}^{0.4} \quad (12)$$

For turbulent flow

$$Nu_{nf} = 0.0059(1.0 + 7.6286\phi^{0.6886} Pe_d^{0.001}) Re_{nf}^{0.9238} Pr_{nf}^{0.4} \quad (13)$$

And for turbulent flow in macro scale, Dittus-Boelter equation [20],

$$Nu = 0.023 Re^{0.8} Pr^{0.4} \quad (14)$$

Pe_d is the particle Peclet number describing the thermal dispersion caused by the microconvection and microdiffusion effects and Pr_{nf} is the nanofluid Prandtl number. Pe_d and Pr_{nf} are defined as

$$\alpha_{nf} = \frac{k_{nf}}{(\rho C_p)_{nf}}, Pr_{nf} = \frac{\nu_{nf}}{\alpha_{nf}}, Pe_d = \frac{u_m d_p}{\alpha_{nf}} \quad (15)$$

Note that the heat transfer correlation described in (12) and (13) were obtained from nanofluid flow in macroscale dimensions. These correlations can be used in the microchannel flow as long as the channel dimension is large enough that scaling effects can be neglected [21].

Similar to heat transfer correlation, limited experimental data are available for the pressure drop in nanofluid flow [14]–[16]. These studies indicated that the existence of nanoparticles in the fluid flow did not cause extra pressure drop when the particle volume fraction is less than 3%. Based

on these experimental observations, pressure drop for nanofluid flow in microchannel can be evaluated using (6) with transport properties of nanofluid.

III. ARTIFICIAL NEURAL NETWORK MODELING

A. Neuron model

A neuron model consists of a processing element [22] with synaptic input connections and a single output. The signal flow of neuron inputs xn_i is considered to be unidirectional as indicated by arrows as in a neuron's output signal flow. A general neuron symbol is shown in Fig. 2.

The neuron's output signal is given by the following relationship

$$o = f(w^t xn) \quad \text{or} \quad o = f(\sum_{i=1}^n w_i xn_i) \quad (16)$$

where w is weight vector defined as

$$w = [w_1 \quad w_2 \quad \dots \quad w_n]^t \quad (17)$$

and xn is the input vector

$$xn = [xn_1 \quad xn_2 \quad \dots \quad xn_n]^t \quad (18)$$

The function $f(w^t xn)$ is often referred to as an activation function. The variable net is defined as a scalar product of the weight and the input vector.

$$net = w^t xn \quad (19)$$

Using (19) in (16), we get

$$o = f(net) \quad (20)$$

It is observed from (16) that the neuron as processing node performs the operation of summation of its weighted inputs. Subsequently, it performs the non-linear operation $f(net)$ through its activation function. Typical activation functions used are [23]

$$f(net) = \frac{2}{1 + \exp(-\sigma net)} - 1 \quad (21)$$

and

$$f(net) = \begin{cases} +1 & \dots \quad net > 0 \\ -1 & \dots \quad net < 0 \end{cases} \quad (22)$$

where $\sigma > 0$ in (21) is proportional to neuron gain determining the steepness of the continuous function $f(net)$ near $net = 0$.

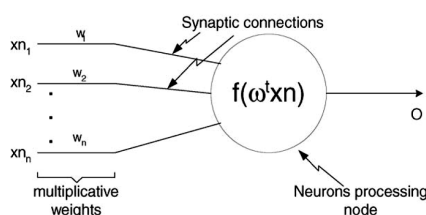


Fig. 2. General symbol of neuron.

By shifting and scaling the bipolar activation function defined by (21) and (22), unipolar activation function can be obtained as [23]

$$f(net) = \frac{1}{1 + \exp(-\sigma net)} \quad (23)$$

and

$$f(net) = \begin{cases} +1 & \dots \quad net > 0 \\ 0 & \dots \quad net < 0 \end{cases} \quad (24)$$

B. Delta learning rule for multi-perceptron layer

The back propagation-training algorithm allows experiential acquisition of input output mapping knowledge within multilayer networks. Input patterns are submitted during the back propagation training sequentially. If a pattern is submitted and its classification or association is determined to be erroneous, the synaptic weights as well as the thresholds are adjusted so that the current least mean square classification error is reduced. The input output mapping comparison of target and actual values and adjustment, if needed, continue until all mapping examples from the training are learned within an acceptable over all error.

During the association or classification phase the trained neural network itself operate in a feed forward manner. However, the weight adjustment enforced by the learning rule propagates exactly backwards from the output layer to the hidden layer towards the input layer. More description and detailed formulation can be found on the study of Singh et al. [23].

IV. RESULTS AND DISCUSSION

A. Analytical approach

Since the Nusselt number correlation for the nanofluid microchannel flow is based on the study of Li and Xuan [14], the Cu-H₂O nanofluid is considered in this study. The particle volume fraction of the nanofluid is in the range of 0.3–2%. Performance of a MCHS using a Cu-water nanofluid in laminar and turbulent flow regimes is discussed below.

A silicon MCHS with the following geometric dimensions $W_{hs} = 1$ cm, $L_{hs} = 1$ cm, $W_{ch} = 100$ μ m, and $L_{ch} = 300$ μ m is considered first. The pumping power is used as a primary variable because it represents the energy consumed during the MCHS operation. Using (5), it is found that the flow in the microchannel remains laminar when the pumping power is under 3 W ($Re < 2000$) and is turbulent for higher powers for this MCHS geometry for example for pump power over 10 Reynolds number is about 20000.

Nusselt number as a function of Reynolds number for laminar flow for three different volume fractions according to (12) is shown in Fig. 3.

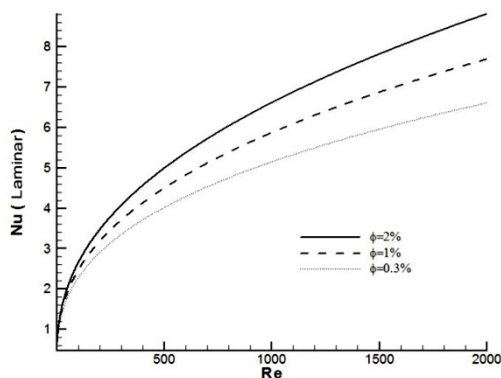


Fig. 3. Nusselt number as function of Reynolds number for laminar flows

It can be seen that Nu increases by increasing ϕ . By comparing Fig. 3 with the diagram of Chein and Huang [1], it is observed that this Nusselt number for small Re is even less than Nu of pure water, therefore this empirical correlation needs correction to be used for microchannels.

Nusselt number for turbulent flow as a function of Reynolds number is shown in Fig. 4. Like laminar flow, by increasing Re and ϕ , Nu increased. In this diagram, Dittus-Boelter correlation for $0.7 \leq Pr \leq 160$ and $Re > 10000$ was used. According to the diagram, an increase of about 20% in Nu is attained using nanofluid.

Using (25) for Nusselt number from [24], the following diagram (Fig. 5) for different volume fractions was produced.

$$Nu_{nf} = 0.04 Re_{nf}^{0.75} Pr_{nf}^{0.333} \quad (25)$$

This method was used by Abbassi and Aghanajafi [25]. The diagram is shown for $\phi=2\%$. By increasing the volume fraction, Nusselt number decreased, thus this method is not a good choice for calculating the Nusselt number of nanofluids in MCHS and needs correction.

In Figure 6, the thermal resistances using the Nu computed before with various pumping powers are shown. It is observed that the minimum R_{th} is $0.045 \text{ K.m}^2/\text{W}$ for $\phi=2\%$ and pump power of 3W. Comparing with the diagram of Chein and Huang [1], a decrease of 75% with the pure water was detected. This reduction in R_{th} is clearly due to the thermal dispersion.

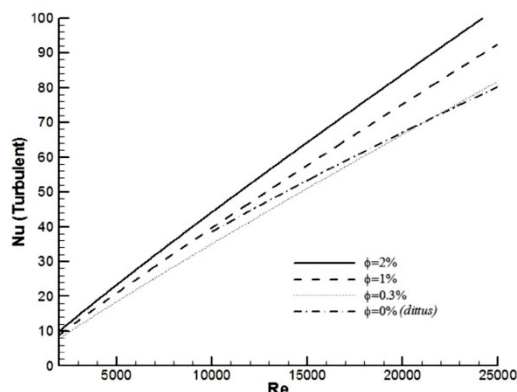


Fig. 4. Nusselt number as function of Reynolds number for turbulent flows

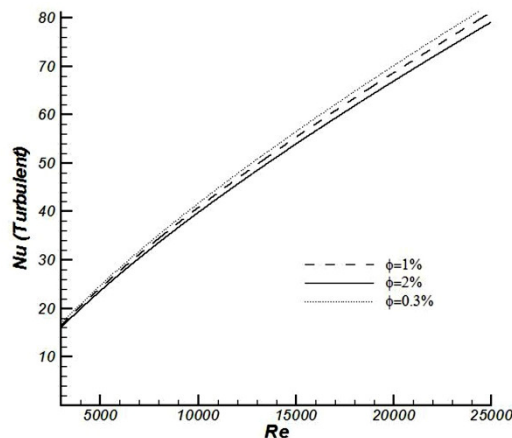


Fig. 5. Nusselt number as function of Reynolds number for turbulent flows using (25)

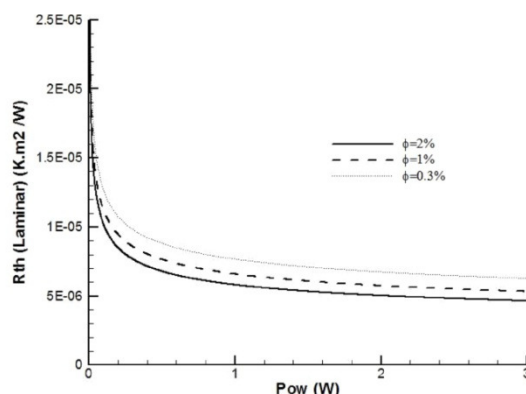


Fig. 6. Microchannel heat sink thermal resistances as function of pumping power for laminar flows

In Fig. 7, the turbulent flow thermal resistances for pump power larger than 3W are shown. It is observed that by increasing pumping power and volume fraction, R_{th} decreases. It is noticeable that the differences among R_{th} with turbulent flow for different volume fractions are less than differences in R_{th} with laminar flow.

In Fig. 8, pressure drops for laminar flow are shown. It has a good congruous with the diagram of Chein and Huang

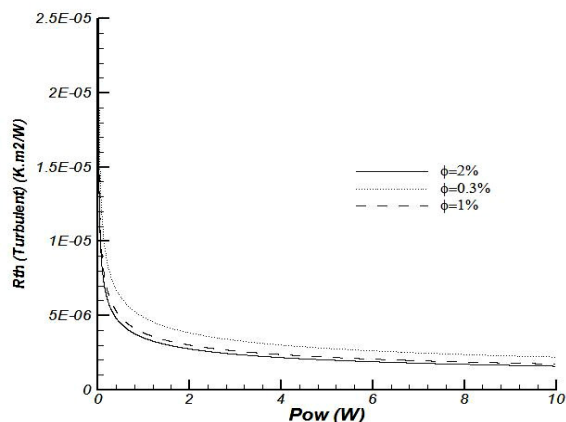


Fig. 7. Microchannel heat sink thermal resistances as function of pumping power for turbulent flows

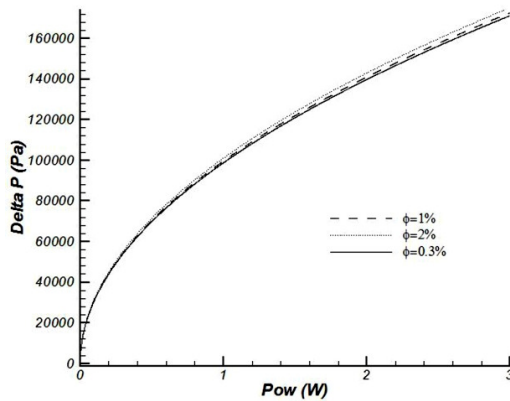


Fig. 8. Pressure drop across microchannel heat sink as function of pumping power for laminar flow

In Fig. 9, pressure drops for turbulent flow are shown. No significant differences existed between the pure water and nanofluid flows because particle size is small and particle volume fraction is low. This may be considered as one of the advantages in using nanofluid as heat transfer fluid in various applications.

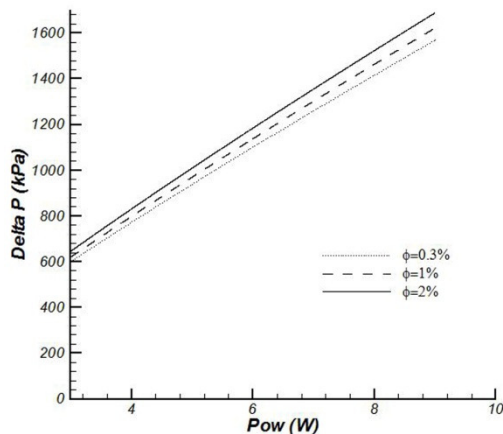


Fig. 9. Pressure drop across microchannel heat sink as function of pumping power for turbulent flows

B. ANN based modeling

An artificial neural network developed here can be used for modeling several geometries of MCHS with several types of nanofluids. This artificial modeling is followed by a computer program which uses ANN for arbitrary geometry and volume fraction range to find the optimum geometry and volume fraction on the basis of minimum thermal resistance. The developed ANN and computer program can be used for a wide range of geometries and nanofluid properties.

A 4-layered network model is taken with [6, 1, 25, 15] configuration i.e. 6 input neurons, 1 output neurons, 25 neurons in the first hidden layer and 15 neurons in the second hidden layer. The input variables are ϕ , L_{ch} , W_{ch} , L_{hs} , Power, t_b and output is R_{th} . In addition, activation functions used for both hidden and output layers are according to (23).

The network is trained using 32000 patterns and 5000 test inputs are given for testing. Training the estimator took about 1000 iterations and about 1.5 h. Performance of the network is 4.0×10^{-9} .

Using this network and the control system, gives the following table which shows the minimum R_{th} for each volume fraction of nanofluids.

Table 1. Minimum R_{th} for volume fraction

Volume fraction	Minimum R_{th} (Km^2/W)
0.01	3.2154 e-06
0.02	2.9035e-06
0.03	2.5972e-06
0.04	2.2939e-06
0.05	2.0922e-06

The above minimum thermal resistances are found with changing the parameters mentioned in Table 2. In these numbers, some limitations such as fabrication and usage are considered.

Table 2. Range of variables for finding the minimum R_{th}

Variable	Range
ϕ	[0.0, 0.05]
L_{ch} (m)	[0.000015, 0.000415]
W_{ch} (m)	[0.000015, 0.000415]
L_{hs} (m)	[0.001, 0.01]
Power (W)	[0.01, 2.5]
t_b	[0.00005, 0.0002]

V. CONCLUSION

The performances of microchannel heat sinks using nanofluids as the coolant were analyzed. The heat transfer and friction coefficients for the nanofluid flow were based on the theoretical models and experimental correlations. For the specific MCHS geometry studied, it is found that nanofluids could enhance MCHS performance as compared with that using pure water as the coolant. The enhancement is due to the increase in thermal conductivity of coolant and the nanoparticle thermal dispersion effect. The other advantage in using nanofluid as coolant in the microchannel heat sink is that there is no extra pressure drop produced since the nanoparticle is small and particle volume fraction is low. In addition thermal resistance of MCHS in turbulent flow was less than laminar flow regime. An optimized geometry was found for every volume fraction using artificial neural network (ANN).

REFERENCES

- [1] R. Chein, G. Huang, "Analysis of microchannel heat sink performance using nanofluids", *App. Thermal Engineering* 25, 2005, pp. 3104-3114.
- [2] H.Y. Wu, P. Cheng, "An experimental study of convective heat transfer in silicon microchannels with different surface conditions", *Int. J. Mass Heat Transfer* 46, 2003, pp. 2547-2556.
- [3] W. Qu, I. Mudawar, "Experimental and numerical study of pressure drop and heat transfer in a single-phase microchannel heat sink", *Int. J. Heat Mass Transfer* 45, 2002, pp. 2549-2565.
- [4] C. Perret, J. Boussey, C. Schaeffer, M. Coyaoud, "Analytic modeling, optimization, and realization of cooling devices in silicon technology", *IEEE Trans. Compon. Packag. Tech.* 23, 2000, pp. 665-672.
- [5] R.W. Knight, D.J. Hall, J.S. Goodling, R.C. Jaeger, "Heat sink optimization with application to microchannels", *IEEE Trans. Compon., Hybrids, Manufact. Technol.* 15, 1992, pp. 832-842.
- [6] A. Horvat, I. Catton, "Numerical technique for modeling conjugate heat transfer in an electronic device heat sink", *Int. J. Heat Mass Transfer* 46, 2003, pp. 2155-2168.
- [7] D.Y. Lee, K. Vafai, "Comparative analysis of jet impingement and microchannel cooling for high heat flux applications", *Int. J. Heat Mass Transfer* 42, 1999, pp. 1555-1568.
- [8] H. Shokouhmand, A. R. Bahrami, "Study of the effects of electrokinetic field on heat transfer through rectangular microchannel", *J. Tehran Univ. College of Eng.* 39, 2005, pp. 773-784.

- [9] Y.S. Muzychka, "Constructal design of forced convection cooled microchannel heat sinks and heat exchangers", *Int. J. Heat and Mass Transfer* 48, 2005, pp. 3119–3127.
- [10] X. Wang, X. Xu, S.U.S. Choi, "Thermal conductivity of nanoparticle-fluid mixture", *J. Thermophys. Heat Transfer* 13, 1999, pp. 474–480.
- [11] S. Lee, S.U.S. Choi, S. Li, J.A. Eastman, "Measuring thermal conductivity of fluids containing oxide nanoparticles", *J. Heat Transfer* 121, 1999, pp. 280–289.
- [12] B.X. Wang, L.P. Zhou, X.F. Peng, "A fractal model for predicting the effective thermal conductivity of liquid with suspension of nanoparticles", *Int. J. Heat Mass Transfer* 46, 2003, pp. 2665–2672.
- [13] Y. Xuan, W. Roetzel, "Conceptions for heat transfer correlation of nanofluids", *Int. J. Heat Mass Transfer* 43, 2000, pp. 3701–3707.
- [14] Q. Li, Y. Xuan, "Convective heat transfer and flow characteristics of Cu-water nanofluid", *Sci. China, Ser. E* 45, 2002, pp. 408–416.
- [15] Y. Xuan, Q. Li, "Investigation on convective heat transfer and flow features of nanofluids", *ASME J. Heat Transfer* 125, 2003, pp. 151–155.
- [16] B.C. Pak, Y.I. Cho, "Hydrodynamic and heat transfer study of dispersed fluids with submicron metallic oxide particles", *Exp. Heat Transfer* 11, 1998, pp. 151–170.
- [17] P. Bhagat, "An introduction to neural nets", *Chem. Eng. Prog.*, 1990, pp. 55–60.
- [18] V. Kurkova, "Kolmogorov's Theorem and multi layer neural networks", *Neural Networks* 5, 1992, pp. 501–506.
- [19] R.P. Lippmann, "Neural Nets for Computing", Lincoln Laboratory, M.I.T, Lexington, MA 02173, U.S.A.
- [20] F.P. Incropera, D.P. DeWitt, "Introduction to Heat Transfer", John Wiley & Sons, New York, 1996.
- [21] H. Herwig, "Flow and heat transfer in micro systems: Is everything different or just smaller?" *Z. Angew. Math. Mech.* 82, 2002, pp. 579–586.
- [22] J.M. Zurada, "Introduction to Artificial Neural Systems", Jaico Publishing House.
- [23] V. Singh*, I. Gupta, and H.O. Gupta, "ANN based estimator for distillation—inferential control", *Chem. Engineering and Processing* 44, 2005, pp. 785–795.
- [24] Zhao CY, Lu TJ. "Analysis of microchannel heat sinks for electronics cooling". *Int J Heat Mass Transfer* 45, 2002, pp. 4857–4869.
- [25] H. Abbassi, C. Aghanajafi, "Evaluation of Heat Transfer Augmentation in a Nanofluid-Cooled Microchannel Heat Sink", *J. Fusion Energy* 25, 2006, pp. 187–196.

\dot{V} coolant volumetric flow rate, m³/s
 w multiplicative weight vector
 w_i multiplicative weight for i th input
 W_{ch} width of microchannel, m
 W_{fin} width of fin, m
 W_{hs} width of microchannel heat sink, m
 xn input vector to neuron
 xn_i i th input to neuron

Greek symbols

α_{nf} nanofluid thermal diffusivity
 λ friction factor of microchannel
 ν viscosity of coolant, kg/ms
 ν_{nf} nanofluid viscosity, kg/ms
 ρ_f density of coolant, kg/m³
 η fin efficiency
 ϕ particle volume fraction
 $(\rho C_p)_p$ particle thermal capacity, kg/m³K
 $(\rho C_p)_f$ pure fluid thermal capacity, kg/m³K
 $(\rho C_p)_{nf}$ nanofluid thermal capacity, kg/m³K

NOMENCLATURE

C_{pf} specific heat of coolant, J/kgK
 D_h hydraulic diameter of microchannel, m
 d_p nanoparticle diameter, m
 $f(\text{net})$ activation function
 G geometric factor of microchannel
 h heat transfer coefficient, W/m²K
 k_f pure water thermal conductivity, W/mK
 k_s material thermal conductivity, W/mK
 k_{nf} nanofluid thermal conductivity, W/mK
 k_p particle thermal conductivity, W/mK
 L_{hs} microchannel heat sink length, m
 L_{ch} microchannel depth, m
 N number of microchannels of heat sinks
 Net scalar product of weight vector and input vector
 Nu Nusselt number
 Pow pumping power of microchannel heat sink, W
 Pe_d nanoparticle Peclet number
 Pr_{nf} nanofluid Prandtl number
 Q Heat to be dissipated, W
 Re Reynolds number based on hydraulic diameter
 Re_{nf} nanofluid Reynolds number
 R_{cap} capacitive thermal resistance, K/W
 R_{con} thermal resistance due to base thickness, K/W
 R_{fin} fin thermal resistance, K/W
 R_{th} heat sink thermal resistance, K/W
 SH particle shape factor
 $T_{w,max}$ maximum heat sink surface temperature, K
 $T_{f,in}$ coolant inlet temperature, K
 u_m averaged velocity in microchannel, m/s